tvst

https://doi.org/10.1167/tvst.8.3.62

Article

Fundus-Controlled Dark Adaptometry in Young Children Without and With Spontaneously Regressed Retinopathy of Prematurity

Wadim Bowl[1], Birgit Lorenz[1], Knut Stieger[1], Silke Schweinfurth[1], Kerstin Holve[1], and Monika Andrassi-Darida[1]

[1] Department of Ophthalmology, Justus-Liebig-University, Giessen, Germany

Correspondence: Monika Andrassi-Darida, Department of Ophthalmology, Justus-Liebig-University, Friedrichstrasse 18, 35392 Giessen, Germany. e-mail: Monika.Andrassi-Darida@augen.med.uni-giessen.de

Received: 24 May 2018
Accepted: 20 March 2019
Published: 28 June 2019

Keywords: dark adaptometry; optical coherence tomography; prematurity; retinopathy of prematurity; macular developmental arrest MDA

Citation: Bowl W, Lorenz B, Stieger K, Schweinfurth S, Holve K, Andrassi-Darida M. Fundus-controlled dark adaptometry in young children without and with spontaneously regressed retinopathy of prematurity. Trans Vis Sci Tech. 2019;8(3):62, https://doi.org/10.1167/tvst.8.3.62

Purpose: We correlate dark adaptation course with foveal morphologic alterations in preterm and term-born children using a modified fundus-controlled perimeter and spectral domain–optical coherence tomography (SD-OCT) imaging.

Methods: We performed fundus-controlled chromatic dark adaptometry in premature children aged 6 to 13 years without retinopathy of prematurity (no-ROP; $n = 61$) and with spontaneously regressed ROP (sr-ROP, $n = 29$), and in 11 age-matched term-born children. The degree of macular developmental arrest (MDA), defined as a disproportion of the outer nuclear layer to inner retinal layers in the fovea (ONL+/IRL-ratio), was analyzed with the DiOCTA tool in SD-OCT scans.

Results: Children with MDA showed a flatter dark adaptation course progression with a significant rod-mediated sensitivity recovery delay (0.0113 vs. 0.0253 dB/s; $P < 0.001$). Preterm-born children with regular foveal morphology reached the final rod-mediated dark-adapted threshold at 12 minutes after bleach at 18.8 dB, compared to after 18.7 minutes at 17.6 dB in children with MDA (no significant difference in final threshold; $P = 0.773$). The cone-mediated dark adaptation progression showed a significant lower final threshold in children with MDA (6.0 vs. 8.1 dB; $P = 0.004$).

Conclusions: Changes in dark adaptation were seen in the presence of MDA observed in premature children in the no-ROP and sr-ROP groups. MDA in former premature children is associated with functional deficits of cone and rod photoreceptor visual pathways.

Translational Relevance: Morphologic alterations in the central retina of premature children, evident in SD-OCT, are associated with long-term functional deficits in the rod and cone pathways, particularly evident in the rod dark adaptation course measured at 12° eccentricity. This indicates a more widespread retinal functional pathology not limited to the fovea, but occurring together with foveal alterations best defined as MDA.

Introduction

Neovascular abnormalities define retinopathy of prematurity (ROP) in the immature retina of preterm born children. Although the disease could be mild and resolves spontaneously in the majority of cases, retinopathy of prematurity (ROP) remains a leading cause of avoidable blindness worldwide.[1] The onset of ROP occurs at preterm ages during a period of rapid development of the rod photoreceptor outer segments.[2] Electroretinographic studies of infants with a history of ROP found significant deficits in rod photoreceptor and rod-mediated postreceptor sensitivity compared to term-born control infants.[2,3]

Interestingly, rod-mediated vision is affected in some children with mild ROP.[3] Specifically, the dark-adapted psychophysical threshold in the parafoveal retina is elevated relative to the threshold in the peripheral retina.[4] In term-born control subjects, the parafoveal and peripheral thresholds are equal.[4,5]

Because the course of development of primate parafoveal rod outer segments is delayed compared to that of peripheral rod outer segments,[6–8] parafoveal rods are less mature than peripheral rod outer segments during the time of active ROP, and possibly more susceptible to the outer segment abnormalities.[4,9]

Full-field studies, however, cannot evaluate specific retinal sites under dark-adapted conditions. Focal dark adaptometry performed with parafoveal stimuli could help close the gap in the assessment of rod-dependent function in children with a history of ROP. Subtle changes under photopic lighting conditions in the foveal and parafoveal area, reported in previous studies,[10] were most accurately evaluated with fundus-controlled perimetry. Unfortunately, dark adaptometry as a practical diagnostic tool is influenced by long test duration, high patient burden, and lack of accurate fixation control. Dark adaptation protocols used in different research projects require up to 60 or more minutes, and typically more than 100 threshold estimates are made. The long duration and a high number of threshold measurements may fatigue some patients and affect reliability.

Recently, we introduced the term macular developmental arrest (MDA) as a description of a shallower foveal pit together with inner and outer retinal changes, a morphologic alteration of the fovea that we observed with higher prevalence in children with a history of prematurity, regardless of the presence of spontaneously regressed ROP (sr-ROP) or not.[11] We defined MDA as the ratio of the outer nuclear layer (ONL) + external limiting membrane (ELM; both assigned as ONL+) to the inner retinal layers (IRL) being 6.5 at maximum. This calculation was used in this study to define groups.

We previously developed a fundus-controlled method for measuring dark adaptation that minimized patient's fixation inaccuracy and maintained sensitivity and specificity of the method.[10] Since parafoveal rod-mediated vision is compromised in former premature children with or without a history of mild ROP, we wanted to test whether there is a more specific correlation of this functional deficit with MDA, and not generally with prematurity. To do so, we tested dark adaptation for the cone and rod pathways, for cones in the center, and for rods at 12° temporal to the foveal center in former premature children with and without MDA. The results of central spectral domain optical coherence tomography (SD-OCT) and dark adaptation course analysis were compared to those of term-born healthy age-similar children.

Methods

Subjects

The present investigation was performed as a part of a long-term follow-up study of prematurely born participants from a prospective multicenter field study conducted between 2001 and 2007.[12] All 90 preterm children included in our study were imaged at the prospective ROP screening study starting at 32 weeks postmenstrual age (PMA) by digital wide-field retinal imaging (RetCam I; Massie Research Laboratories, Inc., Pleasanton, CA), which provides objective documentation of ROP.[12] In our study, only children without apparent psychologic or neuronal disorders, neonatal hypoglycemia, intraventricular hemorrhage, or severe birth asphyxia-related hypoxic-ischemic encephalopathy were included. All children attended mainstream school in the absence of significant deficiencies in basic literacy and numeracy. Parents also were explicitly asked as to early childhood development and performance at school. All perinatal data were available from the original field study. Demographic data and group formation are displayed in Tables 1 and 2. Eleven healthy age-similar term-born children were recruited from the local population who had no history of ocular abnormalities, strabismus, amblyopia, or high refractive errors, and who were capable of performing all tests in this study. The research followed the tenets of the Declaration of Helsinki. Ethical approval was obtained from the local institutional ethics committee (Az 150/09).

Dark Adaptometry

A commercially available Microperimeter MP1 (Nidek Technologies, Padova, Italy) was modified for two-color dark adaptometry, as we described previously.[10] Briefly, a customized external filter holder was placed in front of the objective lens of the MP1 and fitted with optical filters to modify background and stimulus intensities. The filter holder inclined the optical filters in a defined angle (18°) to avoid distracting reflections. Light output of the MP1 was reduced by a thinned long pass filter (Schott RG780; customized material thickness 0.5 mm) for red stimuli and a bandpass filter (Schott BG3; standard material thickness 3.0 mm) for blue stimuli. The thinned Schott RG780 filter showed a full absorption of wavelengths below 600 nm and full transmittance of

Table 1. Demographic Description of Preterm Children Without or With sr- ROP: Distribution of Cohort With sr-ROP

	Preterm-Born Children With sr-ROP	Preterm-Born Children no-ROP[a]	Term-Born Controls	ANOVA, *P* Values
Patients, *n*	29	61	11	–
Age, years; mean ± SD	9.6 ± 1.5	9.3 ± 1.5	9.6 ± 1.3	0.881
Sex, m/f	18/11	28/33	4/7	–
ROP stage, 1/2/3	10/16/3	–	–	–
GA, weeks; mean ± SD	30 ± 2.4	29 ± 4.5	40 ± 0.9	<0.001
BW, gr; mean ± SD	1099 ± 321	1488 ± 332	3664 ± 291	<0.001
BCVA, logMAR; mean ± SD	0.004 ± 0.05	−0.004 ± 0.05	−0.06 ± 0.02	0.021
SER, dpt; mean ± SD	0.6 ± 1.7	0.2 ± 1.5	−0.04 ± 0.3	0.114

[a] No ROP signs during serial screening starting at 32 weeks PMA.

wavelengths above 800 nm. The standard Schott BG3 filter allowed transmission of visible light (>50% transmission from 290–435 nm) and infrared light.

Before the examination, the subject's eye was exposed for 5 minutes to a white Ganzfeld light of 770 cd/m^2, provided by a ColorDome (Espion E2; Diagnosys LLC, Lowell, MA) placed beside the perimeter. Stimuli were presented at six positions of a customized pattern on the posterior pole of the retina (Fig. 1A). Three temporal blue (at 12°) and three central red stimuli (within 2°) on a background of 0.16 cd/m^2 were used in each measurement (Goldmann III size stimuli). As described above, light output to the MP1 was filtered by Schott RG780 and Schott BG3 outside the instrument to create the stimulus colors red and blue. One sequence with three stimuli lasted for 30 to 45 seconds, and was repeated every 2 minutes during the whole session (32 minutes maximum duration; Fig. 1B).

A customized red X, 10° in diameter, was used as the main fixation target. Gaps within the X allowed to project stimuli in the foveal center or at the pericentral position without interfering with the fixation target. A custom software tool exported the raw data from the acquisition computer and plotted the mean measured sensitivity of three blue, respectively three red, stimuli of every sequence in one diagram.

Calculation of the linear gradient of the rapid phase of dark adaptation (S2) was based on the logarithmic curve analysis of the complete curve course (see also the study by Lamb[13]). For each patient a logarithmic adjustment was calculated by a curve analysis tool in MATLAB (MathWorks, Natick, MA). The extreme values of curve pitch changes before and after the rapid phase were automatically recognized. The respective measuring points between the marked extreme values were used

Table 2. Demographic Description of Preterm Children Without or With sr- ROP: Distribution of Cohort According to the Presence of Macular Changes

	Children With Macular Developmental Arrest, MDA	Children With Regular Foveal Morphology, no-MDA	ANOVA, *P* Values
Patients, *n*	43	47	–
age, years; mean ± SD	9.2 ± 1.6	9.6 ± 1.5	0.810
Sex, m/f	26/17	20/27	–
No ROP	27/43	34/47	
ROP Stage, 1/2/3	6/7/3 of 16 sr-ROP	4/9/0 of 13 sr-ROP	–
GA, weeks; mean ± SD	29 ± 2.7	29 ± 2.6	0.712
BW, gr; mean ± SD	1423 ± 439	1330 ± 334	0.337
BCVA, logMAR; mean ± SD	0.02 ± 0.04	−0.02 ± 0.04	0.040
SER, dpt; mean ± SD	0.5 ± 1.6	0.35 ± 1.7	0.275

GA, gestational age; BW, birth weight; BCVA, best-corrected visual acuity; SER, spherical equivalent.

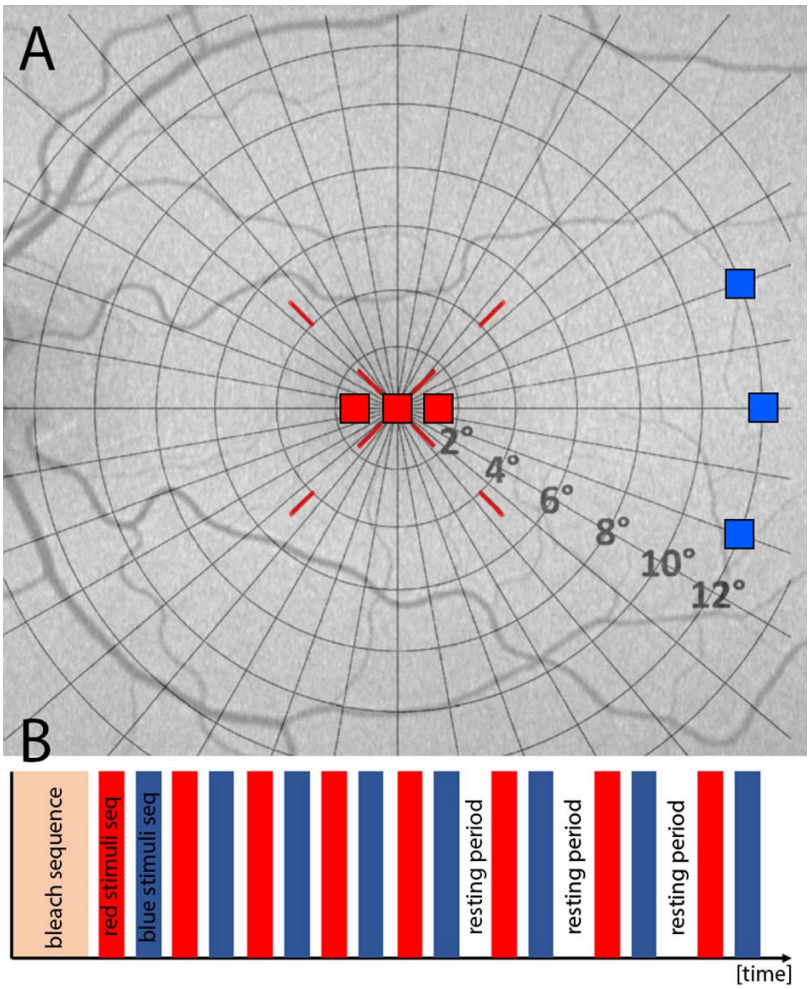

Figure 1. Schematic of the stimuli presented in this study. (A) Stimuli were presented at six positions of a customized pattern on the posterior pole of the retina. Three temporal blue (at 12°) and three central red stimuli (within 2°) on a background of 0.16 cd/m^2 were used in each measurement set, respectively (Goldmann III size stimuli). (B) One sequence with three stimuli lasted for 30 to 45 seconds and was repeated every 2 minutes during the whole session.

for calculating the linear gradient of the rapid phase of dark adaptation. The formula of the rapid phase corresponds to the linear regression formula:

$$y[\mathrm{dB}] = a + (b \times x[\mathrm{sec}])$$

with a determining the intercept and b determining the slope of the linear regression line.

ONL+/IRL-Ratio

High-resolution SD-OCT was performed using Spectralis-OCT (Heidelberg Engineering, Heidelberg, Germany). One eye of each participant was analyzed (matching to the eye in which fundus-controlled dark adaptometry was performed—always the better-seeing or dominant eye). Results of the left eye were mirrored along the vertical axis to be comparable with results of the right eye. For analysis of central thickness, only single scans (B-scan, >80 averaged scans) with the best resolution and best foveal centration were taken into account. Images were exported into a custom automated layer segmentation software[14] (DiOCTA; copyright by Justus-Liebig-University Giessen, Germany), and the thicknesses of the described retinal layers were measured automatically.

We measured the following: retinal nerve fiber layer (NFL); ganglion cell layer plus inner plexiform layer (GCL+IPL); inner nuclear layer plus outer plexiform layer (INL+OPL); ONL+ELM; inner segment plus inner ellipsoid segment of the photoreceptor layer plus outer segment (OS) of the photoreceptor layer (Ellipsoid + OS), and retinal pigment epithelium (RPE). The ratio of ONL+ELM to the sum of inner

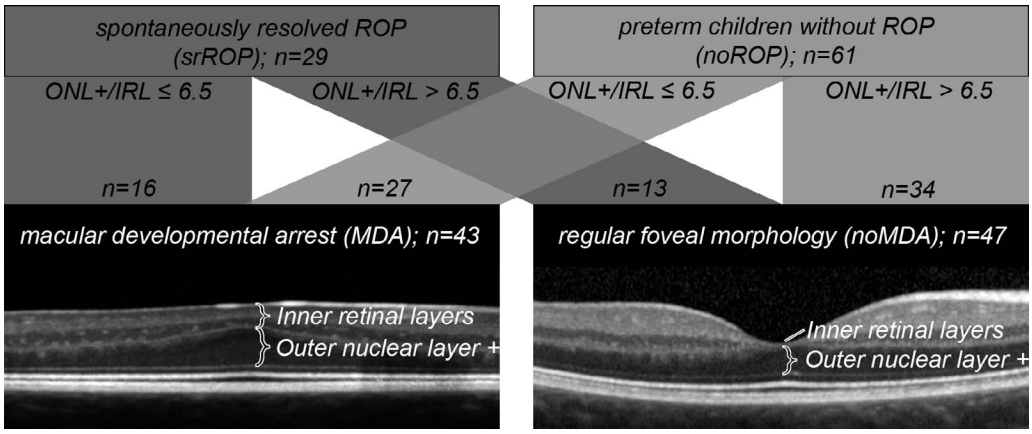

Figure 2. The composition of the preterm-born children groups participating in our study according to ROP in medical history and foveal morphology, as seen with OCT. Macular developmental arrest MDA was defined, in accordance with the study of Bowl et al.,[11] when the ratio between the ONL+ELM and inner retinal layers (ONL+/IRL) was ≤6.5. *Bottom line*: two examples of MDA (left OCT scan) and foveal insemination (right OCTimage). Of note, phenotypic variability concerning the foveal insemination in MDA is high.[11]

retinal layers (NFL+GCL+IPL+INL+OPL = IRL) overlying the foveal center was calculated, as described previously[11] (Figs. 2A, 2B). To elucidate the impact of pathologically changed foveal morphology, the groups were redistributed into groups with an ONL+/IRL-ratio of 6.5 at maximum, defining MDA, and 7 and above as normal foveal morphology (no-MDA).

Statistical Analysis

Statistical analysis was conducted with Sigma Plot 12.0 (Systat Software GmbH, Erkrath, Germany). Normal distribution was tested with the Shapiro-Wilk normality test. Kruskal-Wallis 1-way analysis of variance (ANOVA) on ranks was applied to test for significant differences among the different premature groups and term-born to test for statistical differences between the groups. A Dunn's method was applied as a post hoc test for pairwise comparison. Dynamic curve fitting with polynomial equation was performed to reveal best regression results for the dark adaptation process.

Results

All analyses described below were performed within 101 children aged 6 to 12 years who were capable of undergoing SD-OCT and the fundus-controlled dark adaptometry procedure. All demographic data of preterm-born children with sr-ROP ($n = 29$), preterm-born children without ROP (no-ROP; $n = 61$), and age-similar term-born children (Term; $n = 11$) are described in Table 1. In Table 2, the premature children were classified according to absence or presence of macular developmental arrest MDA, seen in the no-ROP and sr-ROP groups. For sr-ROP, the highest ROP stages seen at the original screening are shown in Table 1. Mean visual acuity was similar in both groups of premature children.

SD-OCT examinations revealed in 16 of 29 sr-ROP and 27 of 61 no-ROP patients with MDA with a shallowed foveal pit coupled with significantly lowered ONL+/IRL-ratio ($P < 0.001$; Fig. 2, lower left image). A total of 47 children ($n = 13$ sr-ROP; 34 no-ROP) showed a normal foveal configuration (no MDA group, Fig. 2, lower right image). Mean retinal thicknesses were significantly higher in the sr-ROP ($P = 0.03$) and no-ROP ($P = 0.05$) groups comparted to the Term group. Accordingly, mean IRL (sr-ROP, $P = 0.013$; no-ROP, $P = 0.034$) and ONL+ELM (sr-ROP, $P = 0.041$; no-ROP, $P = 0.048$) thicknesses were significantly greater in both ROP groups compared to the Term group. Furthermore, significant differences were found even between the sr-ROP and no-ROP groups (no signs of ROP seen during serial screening starting at 32 weeks PMA) in whole retinal thickness ($P = 0.031$), IRL ($P = 0.023$), and ONL+ELM ($P = 0.030$).

When redistributed in MDA ($n = 43$; 16 sr-ROP and 27 no-ROP) and no-MDA ($n = 47$; 13 sr-ROP and 34 no-ROP) groups, the standard deviation was reduced considerably in all analyzed OCT layer parameters (Table 3). The MDA-group showed significant differences in whole retinal ($P < 0.001$), IRL ($P < 0.001$), and ONL+ELM ($P < 0.001$) thickness compared to the no-MDA or Term groups. The no-MDA group showed no significance differ-

Table 3. OCT and Dark-Adaptometry Values of Preterm

	MDA	no-MDA	Term	ANOVA, *P* Value
Foveal SD-OCT layer analysis				
Whole retinal thickness, mean ± SD, µm	270 ± 25	227 ± 17	223 ± 7	<0.001
IRL, mean ± SD, µm	47 ± 25	12 ± 7	12 ± 4	<0.001
ONL+ELM, mean ± SD, µm	127 ± 19	119 ± 11	113 ± 8	0.003
ONL+/IRL-ratio, mean ± SD	3.2 ± 1.3	9.9 ± 1.6	9.7 ± 0.6	<0.001
Dark-adaptation value				
Linear gradient, mean ± SD, dB × sec^{-1}	0.0113 ± 0.011	0.0253 ± 0.008	0.0249 ± 0.006	<0.001
Final rod-mediated threshold, mean ± SD, dB after 30 minutes dark adaptation	17.6 ± 2.2	18.8 ± 1.4	19.2 ± 1.5	0.773
Final cone-mediated threshold, mean ± SD, dB after 30 minutes dark adaptation	6.0 ± 1.7	8.1 ± 1.3	7.9 ± 1.2	0.004

ences to values of term-born children (whole retina, $P = 0.673$; IRL, $P = 0.764$; ONL+ELM, $P = 0.789$). Also, visual acuity was significantly lower in the MDA group (Tables 1, 2; BCVA MDA group, 0.02 ± 0.04; no-MDA group, −0.02 ± 0.04; $P = 0.04$). When distributed according to the highest stage of ROP at screening, there was a trend towards lower VA in children with more severe forms of ROP observed during the initial serial screening starting at 32 weeks of postmenstrual age (Fig. 3). Due to the low number of children per group, it was not possible to calculate significances for this observation.

Figure 4 visualizes the dark adaptation kinetics in the two groups; that is, with normal foveal morphology (no-MDA, $n = 47$; Fig. 4A), and with macular developmental arrest (MDA, $n = 43$; Fig. 4B). For both groups, the cone-mediated sensitivities to red stimuli (red filled area) and the rod-mediated sensitivities to blue stimuli (blue filled area) are shown, highlighting the delayed dark adaptation kinetics in the MDA group.

The dark adaptation curves of exemplary measurements for individual children after bleach are shown in Figure 5A. Preterm-born children with regular foveal morphology reached the final rod-mediated dark-adapted threshold after bleach, measured with blue peripheral stimuli at 12° eccentricity, after a mean of 12 minutes at 18.8 dB. The linear gradient averaged 0.0253 dB/s in preterm-born children with regular foveal morphology and 0.0249 dB/s in term-born age-similar controls. The cone system, described by the reaction to central red stimuli recovered rapidly and reached its final average threshold within 10 minutes at 8.1dB.

Children with MDA showed a flatter course progression with a significant rod-mediated sensitivity recovery delay, expressed by a lowered linear gradient (0.0113 dB/s; $P < 0.001$; Figs. 5A, 5B; Table 3). The final rod-mediated dark-adapted threshold was reached after 18.7 minutes at mean 17.6 dB and showed no statistically significant difference to preterm-born children with regular foveal morphology ($P = 0.773$). The cone-mediated threshold recovered rapidly and was reached after 10.2 minutes but at a significantly lowered mean final threshold of 6.0 dB ($P = 0.004$).

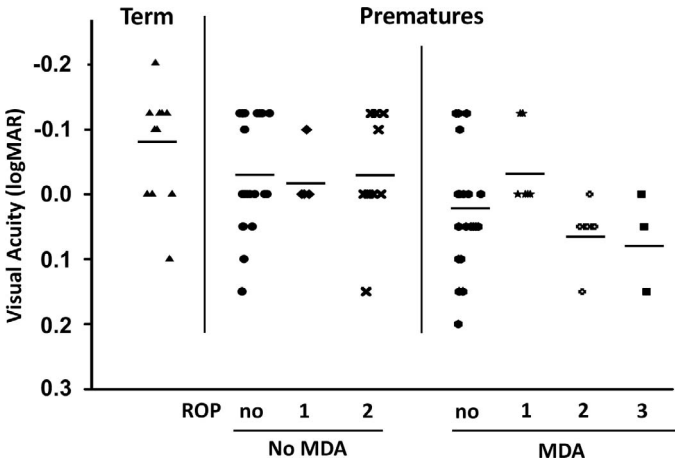

Figure 3. Distribution of visual acuity data among all probands of this study, depending on the presence of MDA and highest stage of acute ROP, and in comparison with age-similar healthy controls. *Status bars*: Mean values in each group.

Discussion

Our study adds evidence to the previously reported results that MDA in preterm born children has an

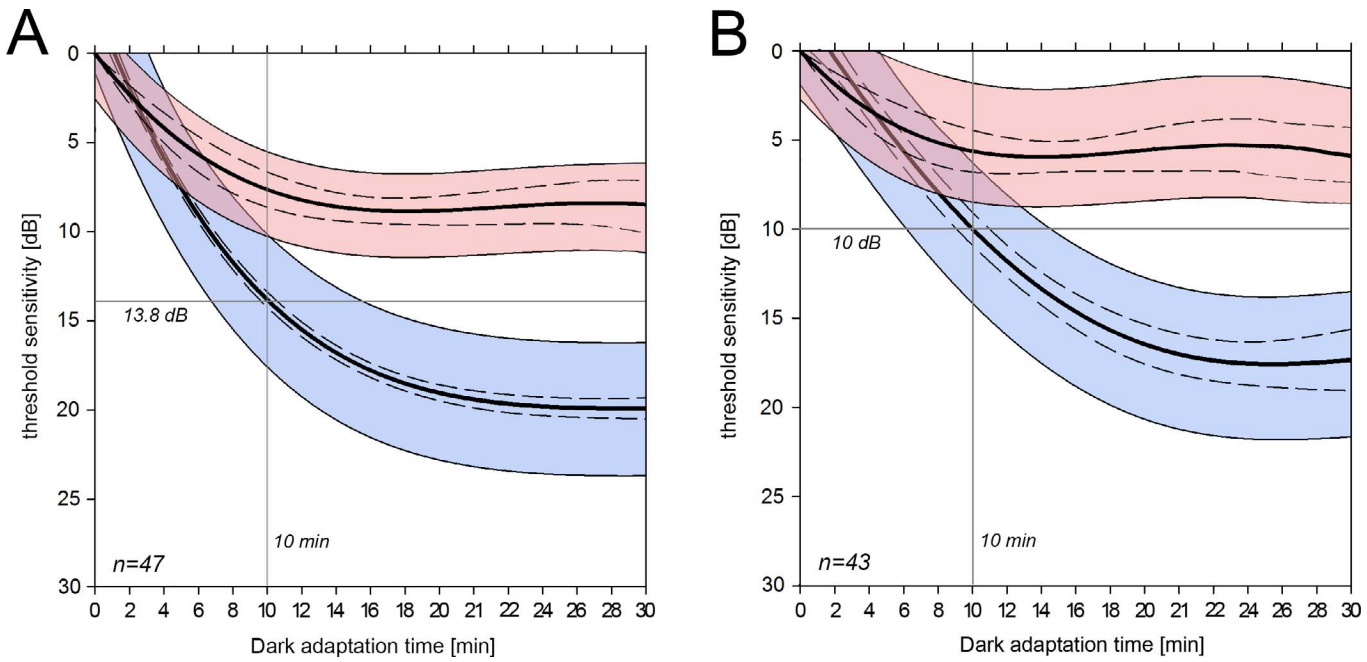

Figure 4. Dark adaptation course measured with a modified fundus-controlled Microperimeter MP1 (Nidek Technology) in preterm-born children with spontaneously regressed or without retinopathy of prematurity divided into the groups normal foveal morphology (no-MDA, $n = 47$; [A]) or macular developmental arrest (MDA, $n = 43$; [B]). In each case, the cone-mediated sensitivity (*red filled area*) to red stimuli and rod-mediated sensitivity (*blue filled area*) are shown. Dark adaptation dynamic fit curve (polynomial 4. order) is shown with 0.95 confidence interval (*dotted lines*) and prediction interval (*continuous outer lines*).

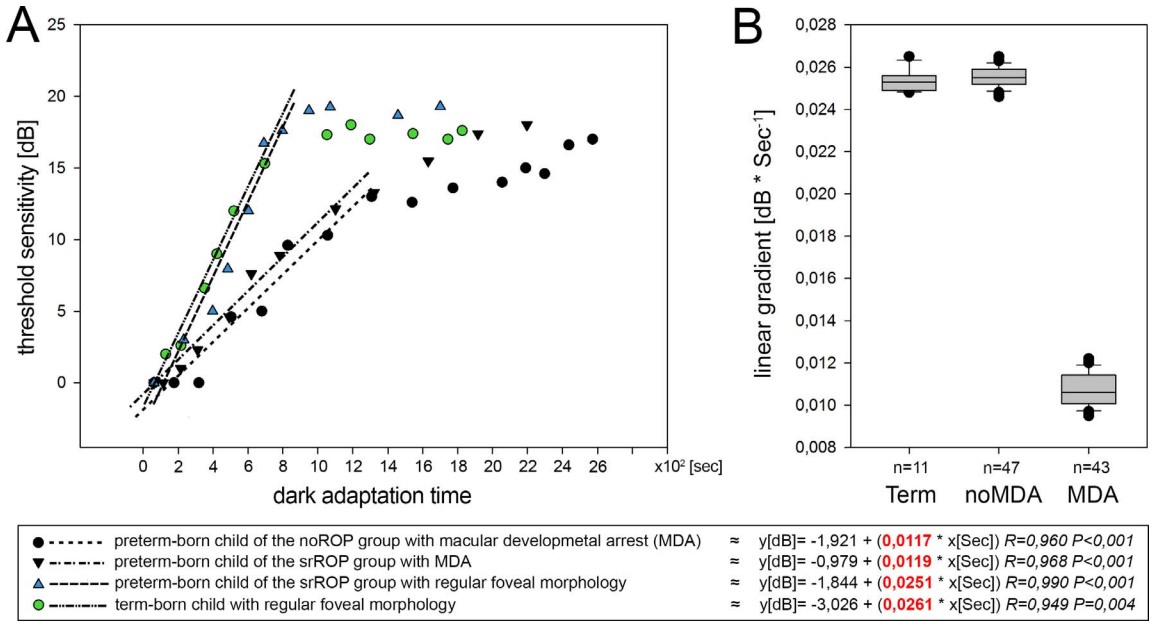

Figure 5. (A) The dark adaptation curves of exemplary measurements for a preterm-born child with MDA and for a preterm and a term-born child with regular foveal morphology (no-MDA). *Lines* mark each of the linear regression curves for each subject. Description of *symbols* and *colors* is given at the bottom of the Figure. (B) Overall linear gradient of the rapid phase of the dark adaptation course of all participating children.

effect not only on the central sensitivity under photopic conditions, but also on the speed of the dark-adaptation process. Others and we have shown a higher incidence of foveal abnormalities in SD-OCT examinations in infants and children with a history of ROP.[11,15–17] It was supposed that the morphologic and functional changes in the central fovea went along with parafoveal changes and impairments of photoreceptors before and on the rod ring at 18° eccentricity.[15] In line with this, affected children tested in our study showed significantly decelerated od-mediated dark adaptation kinetics at 12° temporal to the foveal center, reduced visual acuity, and lowered cone-mediated threshold in the central fovea measured with a recently developed fundus-controlled dark adaptometer.

The process of dark adaptation, or the slow recovery of visual sensitivity after exposure to intense light, is associated with the regeneration of visual pigment.[18] The elevation of the threshold for the detection of visual stimuli depends on the estimated bleach-level of rod and cone photopigments, and follows after a near-total bleach a classic biphasic form, with an early cone-mediated and a later rod-mediated phase.[19] The recovery of the rod-mediated threshold exhibits a region of typical slope across all bleach levels and is termed the S2 component of recovery.[20] It appears that this value is a universal characteristic of dark adaptation recovery in normal (young adult) human eyes and is widely independent of the proportion of the pretest bleach.[21,22] Opsin, produced by bleaching, was proposed to be the substance underlying the S2 component.[22] In healthy human eyes, the rate-limited regeneration of rhodopsin and the S2 component have a common origin in a resistive barrier between a source of 11-cis retinal (RPE) and the opsin molecules in the outer segments. In certain disease states, the rate of regeneration drops to a lower level as a result of reduced enzyme activity. The lowered S2 component in our patient group with MDA resembles findings in patients with early age-related maculopathy[23]or patients with systemic vitamin A deficiency.[24] The final rhodopsin levels expressed as the final visual thresholds in all examined children were entirely average, indicating that the retina is otherwise functioning normally. The underlying morphologic deviations are yet to be clarified.

Our results of altered rod-mediated dark adaptation kinetics are in line with various other studies with electroretinography (ERG), psychophysical, and retinal imaging procedures that showed persistent effects on rod photoreceptor function in ROP children.[3,15,25,26] The new finding is that MDA is the decisive parameter that may be considered as an objective novel biomarker. The critical diameter for spatial summation was shown to be larger in subjects with a history of ROP than in preterm children who never had ROP and term-born controls.[27] This effect was interpreted as evidence of intralaminar reorganization of the postreceptor ROP retina.[27] The critical duration of the light stimulus for temporal summation was longer in subjects with a history of ROP than in preterm children who never had ROP, and was attributed to slow kinetics of activation of rod phototransduction in ROP.[2,27] Particularly interesting are results of an adaptive optics OCT study of the retinal laminae at 18° temporal eccentricity.[28] Akula et al.[28] found a higher ratio of postreceptor to photoreceptor thickness in ROP subjects than in term-born control subjects, which they interpreted as loss or disturbance of photoreceptors and compensation of the retina for altered photoreceptor inputs to the postreceptor retina.[27–29] We observed changed rod-kinetics at 12° temporal eccentricity, which means an area between the central fovea and the rod ring located at approximately 16° to 18°.

The rod photoreceptors are the last retinal cells to mature, except a relatively small number of foveal cones.[27,23] Additionally, the outer segments of the rods central to the rod ring undergo later developmental elongation than those peripheral to the ring, as a result of which dark-adapted visual thresholds central to the ring mature more slowly than those peripheral to the ring.[30] Persistent abnormalities of the intraretinal vasculature were revealed using different OCT-analyses.[15,31] In a longitudinal study of infants with a history of mild ROP, Barnaby et al.[32] found that, even though the clinical disease had resolved spontaneously and entirely by term, dark-adapted visual thresholds showed a protracted course of development that continued until 18 months post-term, whereas in term-born controls the thresholds were mature by the age of 6 months.[32] Matching these results, our measurement of the dark-adapted threshold after 20 minutes showed no statistically significant results between the children with and without morphologically changed fovea.

Reynaud et al.[33] found evidence that the neurosensory retina is involved in the ROP disease process by studying children and rat models of ROP. The escalating metabolic need of rods in the maturity process contributes to ROP. In rat models, rod photoreceptor dysfunction is detectable before vascu-

lar outcome.[27,34,35] It was shown that recovery of the ROP rat's post-receptor retinal sensitivity and retinal vasculature is under the cooperative control of growth factors.[36] In children, there are significant effects on retinal and visual function after the clinical resolution of ROP. In ERG-studies, infants (median 10 weeks) with a history of ROP, showed lower rod and rod-driven postreceptor sensitivity.[3] In children (median 10 years), postreceptor sensitivity normalized but the deficits in rod photoreceptor sensitivity persisted even when the ROP had been mild.[3] These data showed that after clinical healing, the postreceptor neural circuitry undergoes intralaminar reorganization.[37,38] Thus, it appears that rod photoreceptors are involved before, during, and after active ROP.[27] However, our results showed that reduced rod-mediated function may occur even in preterm-born children without ROP. This would indicate that prematurity as such is an important trigger for impaired retinal development involving the macula, that is, MDA.

We showed that cone photoreceptor function (i.e., visual acuity and final threshold after dark adaptation) was reduced in premature children with and without ROP. This difference was statistically significant, in particular in the presence of MDA. In addition, the severity of acute ROP also had a role although there were not enough patients in the different subgroups for statistical analysis (Fig. 3). Previous studies had also shown similar effects on cone function in premature children with and without acute ROP.[39,40] However, at that time no correlation was made with MDA only visible with SD-OCT. It would be interesting to reexamine former patient cohorts with SD-OCT to see whether MDA also correlates with the reported functional deficits in those patients.

We showed, for the first time to our knowledge, a flatter S2 component of the dark adaptation course in young preterm-born children with and without spontaneously regressed ROP in the presence of MDA, but not with normal macular morphology. This demonstrated that MDA not only has significant long-term effects on central cone photoreceptors, affecting central photopic function seen with reduced light increment sensitivity (LIS), but also indicates a more widespread disturbance of rod photoreceptor function up to the morphologic rod ring where rod density is highest. The impairment is substantial and could affect the daily life of children, especially when rapidly changing lighting conditions occur from bright light to darker conditions (e.g., tunnel entries). Considering the findings of previous studies of preterm-born and ROP subjects,[3–5,11,15–17] our present results indicated that persistent malfunctioning of the photoreceptor outer segments may be present in preterm-born children, independent of ROP.

Acknowledgments

Supported in part by a grant from the German Research Council (DFG Lo457/10-1) and in part by a grant from the Else Kröner-Fresenius Stiftung (Project 2015_A131).

Disclosure: **W. Bowl**, None; **B. Lorenz**, None; **K. Stieger**, None; **S. Schweinfurth**, None; **K. Holve**, None; **M. Andrassi-Darida**, None

References

1. World Health Organization. Vision 2020: *Global Initiative for the Elimination of Avoidable Blindness*. Action Plan 2006-2011. Geneva: WHO Library; 2007.
2. Fulton AB, Hansen RM, Moskowitz A, Akula JD. The neurovascular retina in retinopathy of prematurity. *Prog Retin Eye Res*. 2009;28:452–482.
3. Harris ME, Moskowitz A, Fulton AB, Hansen RM. Long-term effects of retinopathy of prematurity (ROP) on rod and rod-driven function. *Doc Ophthalmol*. 2011;122:19–27.
4. Reisner DS, Hansen RM, Findl O, Petersen RA, Fulton AB. Dark-adapted thresholds in children with histories of mild retinopathy of prematurity. *Invest Ophthalmol Vis Sci*. 1997;38:1175–1183.
5. Hansen RM, Fulton AB. Rod-mediated increment threshold functions in infants. *Invest Ophthalmol Vis Sci*. 2000;41:4347–4352.
6. Hendrickson A, Drucker D. The development of parafoveal and mid-peripheral human retina. *Behav Brain Res*. 1992;49:21–31.
7. Dorn EM, Hendrickson L, Hendrickson AE. The appearance of rod opsin during monkey retinal development. *Invest Ophthalmol Vis Sci*. 1995;36:2634–2651.
8. Timmers AM, Fox DA, He L, Hansen RM, Fulton AB. Rod photoreceptor maturation does not vary with retinal eccentricity in mammalian retina. *Curr Eye Res*. 1999;18:393–402.
9. Hendrickson AE. The morphologic development of human and monkey retina. In: Albert DM,

Jakobiec FA, eds. *Principles and Practice of Ophthalmology: Basic Sciences*. Philadelphia: WB Saunders; 1994:561–577.
10. Bowl W, Stieger K, Lorenz B. Fundus-controlled two-color dark adaptometry with the Microperimeter MP1. *Graefes Arch Clin Exp Ophthalmol*. 2015;253:965–972.
11. Bowl W, Stieger K, Bokun M, et al. OCT-based macular structure-function correlation in dependence on birth weight and gestational age-the Giessen long-term ROP study. *Invest Ophthalmol Vis Sci*. 2016;57:OCT235–241.
12. Lorenz B, Spasovska K, Elflein H, Schneider N. Wide-field digital imaging based telemedicine for screening for acute retinopathy of prematurity (ROP). Six-year results of a multicentre field study. *Graefes Arch Clin Exp Ophthalmol*. 2009; 247:1251–1262.
13. Lamb TD. The involvement of rod photoreceptors in dark adaptation. *Vision Res*. 1981;21: 1773–1782.
14. Ehnes A, Wenner Y, Friedburg C, et al. Optical coherence tomography (OCT) device independent intraretinal layer segmentation. *Transl Vis Sci Technol*. 2014;3:1–16.
15. Hammer DX, Iftimia NV, Ferguson RD, et al. Foveal fine structure in retinopathy of prematurity: an adaptive optics Fourier domain optical coherence tomography study. *Invest Ophthalmol Vis Sci*. 2008;49:2061–2070.
16. Villegas VM, Capó H, Cavuoto K, McKeown CA, Berrocal AM. Foveal structure-function correlation in children with history of retinopathy of prematurity. *Am J Ophthalmol*. 2014;158:508–512.e2.
17. Dubis AM, Subramaniam CD, Godara P, Carroll J, Costakos DM. Subclinical macular findings in infants screened for retinopathy of prematurity with spectral-domain optical coherence tomography. *Ophthalmology*. 2013;120:1665–1671.
18. Lamb TD, Pugh EN Jr. Dark adaptation and the retinoid cycle of vision. *Prog Retin Eye Res*. 2004; 23:307–380.
19. Pugh EN. Rushton's paradox: rod dark adaptation after flash photolysis. *J Physiol*. 1975;248: 413–431.
20. Lamb TD. The involvement of rod photoreceptors in dark adaptation. *Vision Res*. 1981;21: 1773–1782.
21. Jackson GR, Owsley C, McGwin G Jr. Aging and dark adaptation. *Vision Res*. 1999;39:3975–3982.
22. Lamb TD, Cideciyan AV, Jacobson SG, Pugh EN. Towards a molecular description of uman dark adaptation. *J Physiol*. 1998;506:88P.
23. Curcio CA, Sloan KR, Kalina RE, Hendrickson AE. Human photoreceptor topography. *J Comp Neurol*. 1990;292:497–523.
24. Cideciyan AV, Pugh EN Jr, Lamb TD, Huang Y, Jacobson SG. Rod plateaux during dark adaptation in Sorsby's fundus dystrophy and vitamin A deficiency. *Invest Ophthalmol Vis Sci*. 1997;38: 1786–1794.
25. Hansen RM, Tavormina JL, Moskowitz A, Fulton AB. Effect of retinopathy of prematurity on scotopic spatial summation. *Invest Ophthalmol Vis Sci*. 2014;55:3311–3313.
26. Hansen RM, Moskowitz A, Tavormina JL, Bush JN, Soni G, Fulton AB. Temporal summation in children with a history of retinopathy of prematurity. *Invest Ophthalmol Vis Sci*. 2015;56:914–917.
27. Moskowitz A, Hansen RM, Fulton AB. Retinal, visual, and refractive development in retinopathy of prematurity. *Eye Brain*. 2016;8:103–111.
28. Ramamirtham R, Akula JD, Soni G, et al. Extrafoveal cone packing in eyes with a history of retinopathy of prematurity. *Invest Ophthalmol Vis Sci*. 2016;57:467–475.
29. Huang WC, Cideciyan AV, Roman AJ, et al. Inner and outer retinal changes in retinal degenerations associated with ABCA4 mutations. *Invest Ophthalmol Vis Sci*. 2014;55:1810–1822.
30. Hansen RM, Fulton AB. The course of maturation of rod-mediated visual thresholds in infants. *Invest Ophthalmol Vis Sci*. 1999;40:1883–1886.
31. Bowl W, Bowl M, Schweinfurth S, et al. OCT angiography in young children with a history of retinopathy of prematurity. *Ophthalmol Retina*. 2018;2:972–978.
32. Barnaby AM, Hansen RM, Moskowitz A, Fulton AB. Development of scotopic visual thresholds in retinopathy of prematurity. *Invest Ophthalmol Vis Sci*. 2007;48:4854–4860.
33. Reynaud X, Hansen RM, Fulton AB. Effect of prior oxygen exposure on the electroretinographic responses of infant rats. *Invest Ophthalmol Vis Sci*. 1995;36:2071–2079.
34. Akula JD, Hansen RM, Martinez-Perez ME, Fulton AB. Rod photoreceptor function predicts blood vessel abnormality in retinopathy of prematurity. *Invest Ophthalmol Vis Sci*. 2007;48: 4351–4359.
35. Liu K, Akula JD, Falk C, Hansen RM, Fulton AB. The retinal vasculature and function of the neural retina in a rat model of retinopathy of prematurity. *Invest Ophthalmol Vis Sci*. 2006;47: 2639–2647.

36. Akula JD, Hansen RM, Tzekov R, et al. Visual cycle modulation in neurovascular retinopathy. *Exp Eye Res*. 2010;91:153–161.
37. Jones BW, Kondo M, Terasaki H, Lin Y, McCall M, Marc RE. Retinal remodeling. *Jpn J Ophthalmol*. 2012;56289–306.
38. Marc RE, Jones BW, Anderson JR, et al. Neural reprogramming in retinal degeneration. *Invest Ophthalmol Vis Sci*. 2007;48:3364–3371.
39. Fledelius HC. Pre-term delivery and subsequent ocular development. A 7–10 year follow-up of children screened 1982–84 for ROP. Visual function, slit-lamp findings, and fundus appearance. *Acta Ophthalmol Scand*. 1996;74:288–293.
40. O'Connor AR, Stephenson T, Johnson A, et al. Long-term ophthalmic outcome of low birth weight children with and without retinopathy of prematurity. *Pediatrics*. 2002;109:12–18.